Effects of the Textile-Sensor Interface on Stitched Strain Sensor Performance

Ellen Dupler
Electrical and Computer Engineering
University of Minnesota
Minneapolis MN USA
duple004@umn.edu

Lucy E. Dunne
Department of Design, Housing, and Apparel
University of Minnesota
Minneapolis MN USA
ldunne@umn.edu

ABSTRACT

The influence of the textile substrate on the performance of a textile-based strain sensor has not been well understood or characterized in many wearable sensor evaluations. The underlying textile has its own anisotropic mechanical behaviors due to its woven or knit fabrication process, and introduces non-trivial structural influences on integrated wearable strain sensors. This study considers stitched strain sensors of two stitch geometries, fabricated on two different knit fabrics, with the sensor stitched in different orientations with respect to the knit structure. The resulting mechanical and electrical performance is characterized under cyclic extension, as the angle of extension (relative to the fabric) is also incrementally changed. The results illustrate a shift from linear to non-linear mechanical behavior as fabric stiffness increases, and variations in behavior between stitch geometries. Results show that force direction and sensor placement both introduce variability in calculated elastic modulus, which affect sensor modeling (e.g. predicting applied force from sensor response). A novel stitch geometry (the chainstitch sensor) is characterized as having a higher gauge force and lower transverse sensitivity factor than the coverstitch sensor. This work offers insight into the textile-sensor interface and design implications for development of textile-based sensors.

CCS CONCEPTS

• User/Machine Systems: Human factors • Robotics: Sensors.

KEYWORDS

E-textile; strain sensor; textiles; wearable technology; smart clothing; wearable sensor.

ISWC '19, September 9–13, 2019, London, United Kingdom © 2019 Association for Computing Machinery.
ACM ISBN 978-1-4503-6870-4/19/09…$15.00
https://doi.org/10.1145/3341163.3347717

ACM Reference format:

Ellen Dupler and Lucy E. Dunne. 2019. Effects of the Textile-Sensor Interface on Stitched Strain Sensor Performance. In *Proceedings of ACM ISWC conference (ISWC'19). ACM, New York, NY, USA,* https://doi.org/10.1145/3341163.3347717

1 Introduction

Monitoring biomechanical forces and strains noninvasively is a perennial wearable sensor research challenge, due to the tradeoff between promoting sensor comfort and promoting sensor performance (high accuracy, low noise and error, repeatability, etc.). The relatively large elongations induced by body motion limits thin film strain sensors and electronic skin proposals, while poor accuracy and repeatability limits many textile-based strain sensors from being commercially viable. There are many approaches to solving this challenge, including: using a multiplicity of sensors for redundancy [13], using fiber-type sensors [11,14] or other novel textile sensors [20], increasing the stretchability of thin film sensors [1], and decreasing the flexibility of textile-based sensors (stiffer interconnects, encapsulation, etc.) [4].

Other proposals look at further understanding the complexity of textile-based sensors to optimize parameters and improve performance. Related work has explored knitted sensors [6,17,18], and considered the effects of knit types [5] or knit structure variables [2,19] to improve strain sensor electro-mechanical performance. Stitched sensors in particular offer advantages for wearables in their ability to be applied to a wide range of textile substrates, and to be integrated in unconstrained geometries (as opposed to woven or knitted forms). For stitched sensors specifically, the effects of conductive yarn variables and stitch placement on sensor performance have been explored for stretch sensors [16] and fabric RFID tags [12,15]. This work aims to increase the electro-mechanical understanding of stitched textile-based strain sensors, in order to inform textile strain sensor design.

Gioberto and Dunne [7,8] introduced a garment-integrated strain sensor that is stitched onto a textile substrate and operates via a variable conductor path principle. The sensor is formed by floating a looped conductive thread on one side of a textile substrate using a sewing machine. As the fabric stretches, the deformation causes contact points in the conductive path to shift, and the overall length (resistance) of the conductive path changes accordingly. This

sensor is influenced by the mechanics of the textile substrate, because the textile must first be deformed in order to induce changes in the sensor structure. Previous work observed that the fabric choice could influence sensor performance [9,10]. The current work investigates the stitched sensor performance as a result of the fabric substrate, stitch geometry, and angle of applied force to illuminate key textile-sensor interactions.

2 Methods

Stitched strain sensors were fabricated using two stitch geometries, on two knit substrates, with three specimens per sample group. The ISO #406 two-needle bottom coverstitch (Figure 1, right) was selected because of its demonstrated success as a sensitive and repeatable sensor over strain ranges 0% to 50% [3]. The ISO #401 chainstitch (Figure 1, left) was selected because promising pilot testing performance indicated its high sensitivity and low transverse sensitivity. Shieldex® Conductive Twisted Yarn Silver Plated Nylon 66 Yarn 235/34 dtex 4-ply was used as the bottom looper thread and typical cotton/polyester thread served as the top needle thread(s) for both sensors. Sensors were sewn using an industrial coverstitch machine (Juki MF-7723 high-speed, flat-bed). The chainstitch is sewn by removing one of the needles.

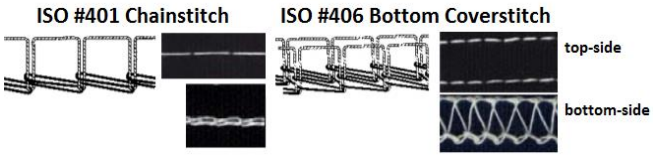

Figure 1: Sensor stitch geometries used for testing: (Left) ISO #406 Bottom Coverstitch, (Right) ISO #401 Chainstitch. Adapted from [21]

This study evaluated fabrics typically used for sensing garments. 4-way and 2-way stretch weft knits make up the majority of close-fitting athleisure apparel, so a representative sample from each category was picked. A double knit structure, in which two weft knits are interlocked together, was selected because it offers greater stability and easier sewability (Figure 2, left and center). A polyester/Spandex 4-way stretch double knit ("scuba knit") elastomeric fabric with ~63% elongation in both directions with full recovery and a 100% polyester 2-way stretch double knit ("ponte knit") fabric with ~50% crosswise and 6% lengthwise elongation with near full recovery were selected as the test textile substrates.

A 7cm sensor length was chosen because it was comparable to commercial sensors (StretchSense^{TM}) and appropriate with anthropometric joint lengths. The fabric was cut into 12.7cm squares (to accommodate 7cm sensors) using preparation recommendations from ASTM D4964 and the stiffest direction was marked as the reference 0°. Sensor orientation in relation to the different knit stretch directions was an important sample variable. Because these knits are both weft knits (the most common), they have perpendicular wales and courses. Assuming the knit is symmetric around the center point, sensors were sewn at 5 angles: 0°, 30°, 45°, 60°, and 90° (Figure 2, right). Each sensor measured 3.5cm around the center of the sample, and was secured on both ends with a male metal crimp snap connector, which also served as attachment points for the electrical leads (Figure 3). The average resistance was 10.9Ω for the coverstitched sensors and 7.7Ω for the chainstitched sensors.

Figure 2: (Left) Weft Knit Structure, (Center) Double Knit/Interlock Stitch, (Right) Sensor Placements

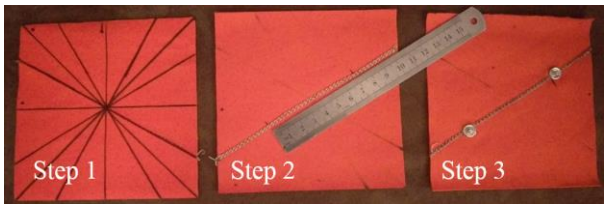

Figure 3: Stitched stretch sensor fabrication sequence (chainstitch on 4-way fabric, 60° shown). Adapted from [21]

In total, the substrate, stitch geometry, and stitch angle variables resulted in 22 sample groups (2 fabric-only + 20 fabric+sensor) and 66 total specimens used for testing.

An Instron 3365 constant-rate-of-elongation test machine equipped with Bluehill 3 software was selected to conduct the controlled uniaxial displacement test and collect force, displacement and voltage measurements for this study. A Wheatstone bridge circuit was constructed with the sensor (with 3Ω to 10Ω +/-5% reference resistors) and the bridge voltage was captured with the Instron transducer. The sensor specimens were clamped into the pneumatic grips (80psi used to prevent fabric slippage) in a grab method setup and the first cycle was used as a preconditioning step. The strain range was set to 0% to 30% at a strain rate of 200mm/min. All testing was conducted in indoor lab space with temperatures in the general range of 20°C to 23°C, humidity 16% to 24%.

Three subsequent elongation and relaxation cycles were used for data analysis and measurements were sampled at 50Hz. Matlab R2019a software was used primarily for data analysis and regression fitting.

2.1 Test Methodology

The test battery was arranged into three phases. The aim of the first phase was to characterize the influence of sensor fabrication on the textile substrate's mechanical behavior. To determine this, the mechanical properties for both fabric substrates alone and fabric+sensor specimens were compared. Additionally, the change in mechanical properties due to force angle (uniaxial force axis with respect to the knit structure 0°) in both of these conditions were

compared. This is important for calibrating the sensor elongation with the applied force.

The second phase considered the influence of sensor geometry and sensor orientation relative to the knit substrate on electrical sensor performance. Sensors sewn onto the fabric at 0°, 30°, 45°, 60°, and 90° from the textile reference 0° were subjected to uniaxial force applied inline with the sensor (Figure 4, left). This angle refers to both force direction (testing fabric only) and the stitch angle (the sensor placement when testing fabric+sensor). Then the sensors' performance in regards to their placement and stitch geometry were compared. Gauge factor, linearity errors and other variables are calculated to characterize the sensor behavior (see Section 2.2).

The third phase focused on comparing transverse sensitivity of the each sensor. This transverse sensitivity factor (K_T) is heavily influenced by sensor geometry and directional sensors typically have one dimension (length) significantly larger than the other (width). All specimens were subjected to uniaxial forces directed at 4 angles, (30°, 45°, 60°, 90°) with respect to the sensor axis/stitch angle and compared to its performance to when the force was in-line (0°). One example setup can be seen in Figure 4, right.

Figure 4: (Left) 4-way knit, 0° Coverstitched Sensor, 0° Force (Right) 2-way knit, 60° Chainstitched Sensor, 60° Force

2.2 Mechanical & Sensor Performance Variables

The mechanical properties are characterized by the force range and the elastic modulus. The force range, ΔF, is defined as the amount of force required to elongate to the maximum displacement. Due to the knit structure, the stiffness and force ranges varies with force angle. The elastic modulus, E is calculated from the primarily linear relationship between the stress=f(strain) of the elongated sensor and fabric. A linear fit of the form y=mx+b is generated from the Force=f(Displacement) data and the linear slope E is found using the sensor length, d_o, the displacement divided by the original length, ε, and the fabric area between the clamps, A as follows:

$$E = \frac{stress}{strain} = \frac{F/A}{d/d_o} = \frac{d_o}{A} \cdot \frac{F}{d}$$

In this case, the area between the tensile tester grips is assumed to be constant between the width of the grips and that the stress is limited to this area. This is only an approximation, since the grip test method allows fabric to exist beyond the width of the grips.

The linearity error (R^2, measuring linear fit) and the root-mean-square error (RMSE, measuring the quality-of-fit) were calculated for the stress-strain regression model. For these purposes, only the elongation portions of the curves were used.

The stitched sensor exhibits piezoresistive behavior. The sensor resistance is calculated from the measured Wheatstone bridge voltage V_B and the supply voltage V_S as follows:

$$R_1 = R_2 = R_3, \qquad R_x = \frac{R + 2R(V_B/V_S)}{1 - 2(V_B/V_S)}$$

The resistance at zero extension is used as the nominal resistance and decreases thereafter for these sensors, so the maximum change from nominal resistance is considered the peak-to-peak change. This maximum was averaged for each specimen (S1, S2, S3) in the sample group to calculate an Average Peak-to-Peak Change in Resistance, also called the sensor response or resistance range and shown in absolute terms (Ω) or normalized (%).

The normalized change in material property divided by the normalized strain is called the sensitivity or gauge factor (GF). For the stitched strain sensors, the known property change is resistance for a given tensile strain, R=f(strain), so that:

$$Gauge\ Factor = [\Delta R/R]/[\Delta L/L]$$

The GF was calculated from plotting normalized change in resistance vs strain from measurements. A linear fit is generated, with the slope representing the GF. This variable is ~2 for most traditional strain sensors, but varies with other soft sensors.

The sensor response linearity (R^2) and RMSE was also calculated, because deviations from the desired fit can indicate non-negligible variable effects, large hysteresis, large degrees of error, or permanent deformation.

Dynamic baseline drift (describing how much the sensor response at zero extension drifts over consecutive cycling) is also included. This is different from static baseline drift, which is how much the sensor resistance changes under static extension. Each test condition includes three elongation/relaxation cycles, so the difference in resistance at zero extension from the final cycle vs the initial cycle is calculated and averaged for each sample group. The recovery behavior of both the sensor and fabric substrate influences this value, which is ideally as close to zero as possible.

As previously mentioned, the above values were all calculated from linear regression fits of the *elongation curve only*. In contrast, calculating the average hysteresis error uses data from the entire cycle (both elongation and relaxation curves). The hysteresis error here was calculated by finding the maximum difference between the curves for every displacement value (Figure 5). To simplify calculations, only data from the final cycle for each specimen is used.

$$\overline{Hysteresis\ Error} = \frac{|Y_{iR} - Y_{iE}|}{|Y_{d=max} - Y_{d=min}|}$$

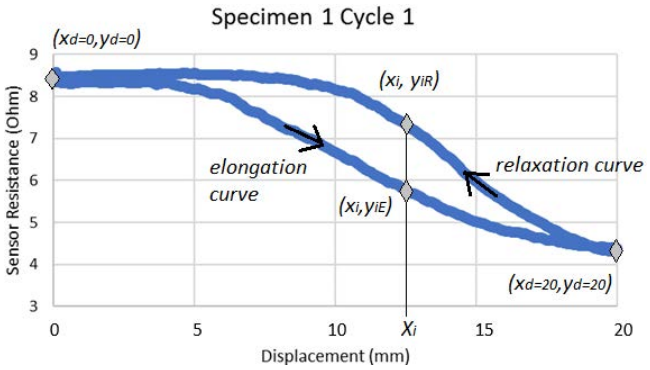

Figure 5: Defining points used in hysteresis calculation. Reprinted from [21]

Ideally the sensor would ignore forces in any direction other than its main orientation but in reality, the sensor may be responsive to offset forces. This is represented by the transverse sensitivity factor, K_T, a ratio of sensitivities calculated from different force directions. (As will be explained in the results, the transverse direction was redefined from the traditional 90° to 60°).

$$K_T = \frac{GF(transverse\ direction)}{GF(axial\ direction)}$$

3 Results & Discussion

The results follow the order of the 3 phases of our test battery. Mechanical characteristics are presented first (comparing force ranges and elastic modulus of the knit-only with the knit+sensors for the 4-way knit and the 2-way knit). Then the electrical properties of the stitched stretch sensor sample groups, as described above, are characterized and presented in Table 2. Finally, the transverse sensitivity factors for the tested offset forces are presented.

3.1 Mechanical Characterization

As seen in Figure 6, the force ranges for the 4-way knit sample groups were within the same order of magnitude and show the expected slight decrease from the stiffest direction (0°) to the least stiff (90°). The presence of the stitched sensor also generally increases the apparent stiffness of that force direction. The only exception to this is the 0° coverstitched stretch sensor, which shows a 10% decrease in stiffness.

The 2-way knit sample groups were expected to require greater forces to elongate the stiffer directions at the maximum 30% strain, but the near exponential increase in force is the key observation (Figure 7). This resulted in nonlinear force-displacement behavior for the stiffer fabric directions (0° to 45°), shown in Figure 8.

The presence of the stitched sensor increases the apparent stiffness in the stretchier 2-way knit directions, but decreases the stiffness of the stiffer fabric directions. For both knit types, the chainstitch geometry constrained elongation more than the coverstitch. Since this stitch geometry itself stretches visibly less than the coverstitch, this is not surprising. The coverstitch geometry has a cross-looped structure which affords easier elongation. The decreases observed in the stiffest fabric directions are potentially due to gaps created by needle holes that decrease stiffness beyond a certain threshold.

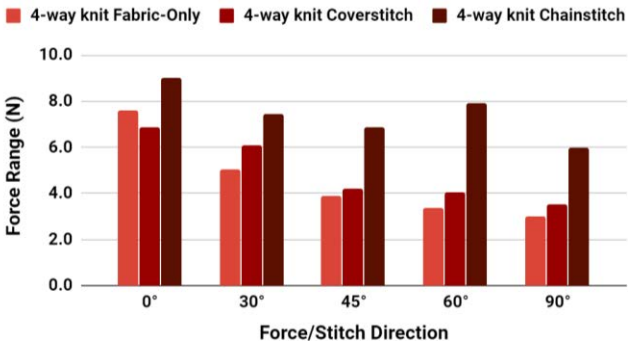

Figure 6: Force Range of 4-way Knits With and Without Sensors. Adapted from [21]

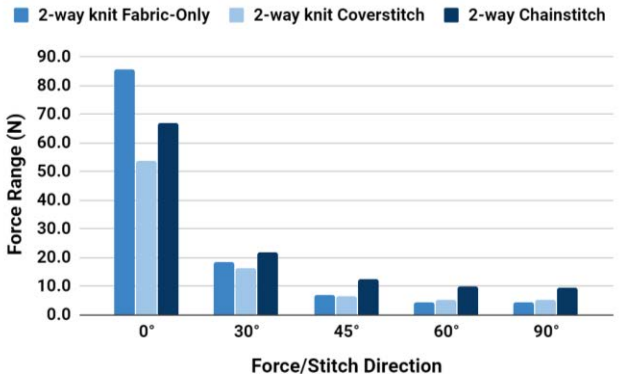

Figure 7: Force Range of 2-way Knits With and Without Sensors. Adapted from [21]

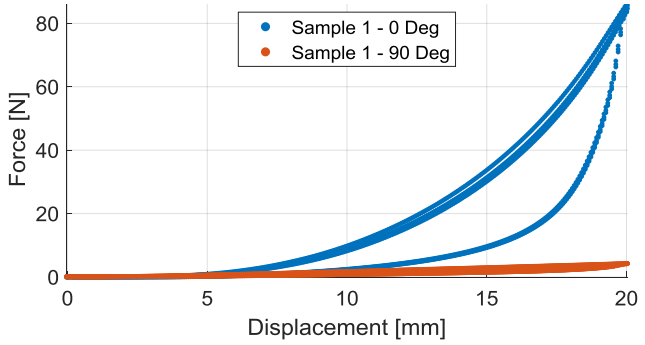

Figure 8: Full Elongation/Relaxation Cycle for the Stiffiest and Stretchiest 2-way Knit Fabric Directions

Looking more closely at individual force responses for each of the sensor groups, it's clear that two sample variables seem to induce nonlinear force-displacement curves: when the force angle or sensor orientation is aligned along the 2-way knit stiffer directions, and when the chainstitch geometry experiences strains of more than

~21% (displacement of more than 15mm, Figure 9). The linear regressions for these groups have lower R^2 values and higher RMSE errors. All other test parameters yielded a more linear force-displacement relationship.

The range of measured elastic moduli is shown in Table 1 and highlights the importance of this investigation and the influence of both fabric choice and sensor stitch geometry on estimating real forces. The elastic moduli for the fabric+sensors ranged from 61% to 205% of the fabric-only values, presenting a challenge in using the sensors to predict absolute force values.

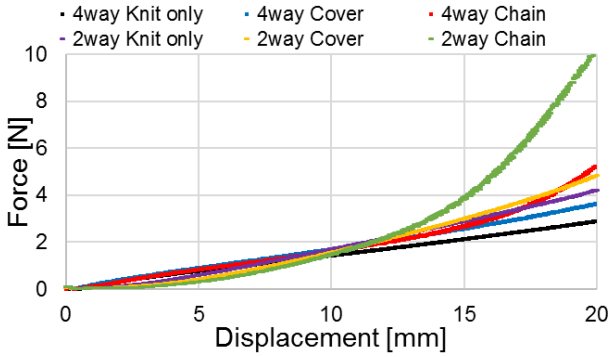

Figure 9: Elongation Only Force (Displacement) Plot for 2-way 90° Coverstitch and Chainstitch Sample Groups

Sample Group	E (N/mm)	Degree from 0°				
		0°	30°	45°	60°	90°
4-way Fabric	E(0°)	0.00779	0.00495	0.00372	0.00318	0.00283
2-way Fabric	E(0°)	0.0722	0.0156	0.00668	0.00445	0.00442
4-w Coverstitch	% of fabric only E(0°)	92%	124%	115%	126%	121%
4-w Chainstitch		112%	136%	162%	204%	175%
2-w Coverstitch		61%	88%	91%	113%	119%
2-w Chainstitch		77%	114%	149%	188%	183%
Color guide:		*+/- 0-20%*	*+/- 21-40%*	*+/- 41-61%*	*+/- 61-80%*	*+/- 81-100%*

Table 1. Calculated Elastic Modulus (N/mm) of Samples. Reprinted from [21]

3.2 Electrical Characterization, Force Inline

The sensor performance of all sample groups is summarized in Table 2, and each variable is discussed here in further detail.

A characteristic ΔResistance vs Displacement plot is shown in Figure 10, with the most deviation from linearity typically in the beginning plateau. The chainstitch sample groups had a similar plateau but larger hysteresis and resistance change than shown.

Figure 11 shows that the gauge factors (GF) for sensors with the chainstitch geometry were approximately twice as large as those of the coverstitch (-2 compared to -1). Although it was clear that the fabric stiffness varied with angle, the GF interestingly didn't show much variation based on sensor orientation on the fabric ("stitch angle") and was influenced more by sensor stitch geometry. The 2-way knit chainstitch sample group shows the highest GF (-2.24) and the 2-way knit coverstitch sample group shows the least (-1.01). As a reference, a GF of +/-2 is generally acceptable value for many strain sensors.

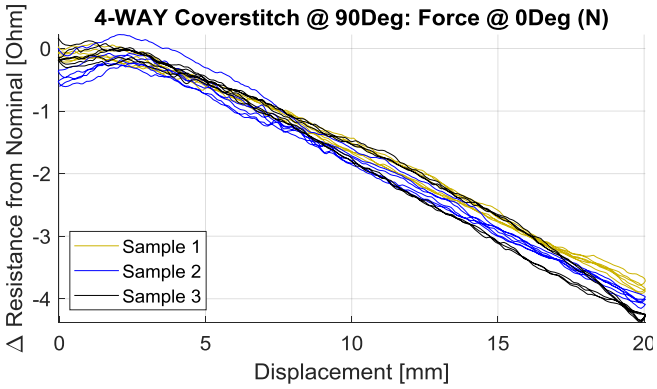

Figure 10: Characteristic ΔResistance (Displacement) Plot (4-way 90° Coverstitch Sample Group)

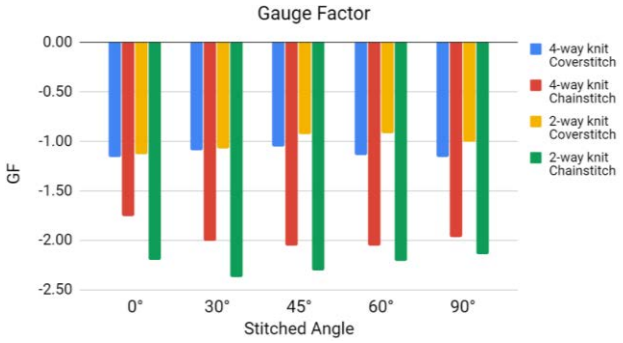

Figure 11: Gauge Factor of Stitched Sensors. Reprinted from [21]

The linearity R^2 error values for all sample groups are similarly high (~0.95+) except for the 2-way knit coverstitch sewn at the 45° and 90° directions (~0.88). It's believed that the increased width of this stitch allows offset forces to cause undesirable variations in the sensor response when placed in these fabric directions. For the 2-way knit, the difference between preferential stretch direction is more extreme, so the knit structure while stretching may be more influenced by these shear forces compared its 4-way knit counterpart (which has better elasticity).

Regarding RMSE, the 4-way knit coverstitch has the least error (0.11Ω) while the 2-way knit chainstitch has the most (0.046Ω), although all groups had errors less than 0.05Ω compared to the overall change of 4Ω over the full strain range. Although nonlinear behavior was observed mechanically, linear regressions for Resistance vs Strain seem to match the sensor response well.

Sample Group	Calculations	Degree from 0° of Knit the Sensor was Stitched				
		0°	30°	45°	60°	90°
4-way knit Coverstitch	**Sensitivity/GF**	**-1.15**	**-1.09**	**-1.05**	**-1.14**	**-1.16**
	% of GF(0°)	100%	95%	91%	99%	101%
	Fit Line R^2	*0.956*	*0.966*	*0.973*	*0.976*	*0.983*
	Fit Line Avg RMSE (Ω)	*0.0184*	*0.0146*	*0.0134*	*0.0132*	*0.0114*
	Hysteresis Error (Ω)	*0.81*	*0.46*	*0.36*	*0.29*	*0.35*
	Baseline Drift (Ω)	*-0.513*	*-0.088*	*-0.060*	*-0.043*	*-0.0474*
	Transverse** GF	-0.090	-0.548	-0.545	-0.574	-0.616
	Trans sensitivity factor, K_t	8%	50%	52%	50%	53%
4-way knit Chainstitch	**Sensitivity/GF**	**-1.76**	**-2.00**	**-2.05**	**-2.06**	**-1.96**
	% of GF(0°)	100%	114%	117%	117%	112%
	Fit Line R^2	*0.945*	*0.977*	*0.973*	*0.969*	*0.960*
	Fit Line Avg RMSE (Ω)	*0.0316*	*0.0237*	*0.0264*	*0.0285*	*0.0303*
	Hysteresis Error (Ω)	*1.29*	*1.64*	*1.51*	*1.35*	*1.49*
	Baseline Drift (Ω)	*-0.089*	*-0.023*	*-0.050*	*-0.045*	*-0.0179*
	Transverse** GF	-0.081	-0.303	-0.189	-0.193	-0.207
	K_t	5%	15%	9%	9%	11%
2-way knit Coverstitch	**Sensitivity/GF**	**-1.13**	**-1.07**	**-0.93**	**-0.92**	**-1.01**
	% of GF(0°)	100%	95%	82%	82%	89%
	Fit Line R^2	*0.949*	*0.964*	*0.887*	*0.951*	*0.879*
	Fit Line Avg RMSE (Ω)	*0.0202*	*0.0157*	*0.0245*	*0.0146*	*0.0278*
	Hysteresis Error (Ω)	*0.28*	*0.43*	*0.52*	*0.44*	*0.44*
	Baseline Drift (Ω)	*-0.131*	*0.116*	*0.112*	*-0.005*	*-0.0234*
	Transverse** GF	-0.765	-0.707	-0.768	-0.816	-1.006
	K_t	68%	66%	83%	88%	100%
2-way knit Chainstitch	**Sensitivity/GF**	**-2.20**	**-2.37**	**-2.31**	**-2.21**	**-2.14**
	% of GF(0°)	100%	108%	105%	100%	97%
	Fit Line R^2	*0.933*	*0.954*	*0.948*	*0.934*	*0.941*
	Fit Line Avg RMSE (Ω)	*0.0455*	*0.0402*	*0.0414*	*0.0454*	*0.0413*
	Hysteresis Error (Ω)	*1.62*	*1.84*	*1.73*	*1.65*	*1.17*
	Baseline Drift (Ω)	*0.041*	*-0.058*	*-0.082*	*-0.039*	*-0.0297*
	*Transverse** GF*	*-0.016*	*-0.083*	*-0.149*	*-0.072*	*-0.283*
	K_t	1%	3%	6%	3%	13%
GF Color guide:		*+/- 0-5%*	*+/- 6-10%*	*+/- 11-15%*	*+/- 16-20%*	*+/- 21-25%*
Transverse GF Color guide:		*+/- 0-10%*	*+/- 11-20%*	*+/- 21-40%*	*+/- 41-60%*	*+/- 61-100%*

Table 2. Summary of Sensor Performance based on Sensor Placement with respect to the Knit Structure. Reprinted from [21]

The baseline drift was highest (|0.11|Ω+) along the stiffest fabric direction (0°) and decreased thereafter (avg -0.023Ω). This is probably due to the imperfect elastic recovery in these directions over progressive cycling, and the 4-way knit 0° coverstitch has an especially high drift (-0.513 Ω). Most baseline drifts occurred in the negative direction (the same direction as elongation).

The hysteresis error is also more dependent on stitch geometry, and is larger for the chainstitch groups. This error is similar across all the sensor placements/stitch angles, with an average of 0.44Ω for the coverstitch groups and 1.53Ω for the chainstitch groups.

3.3 Electrical Characterization, Force Offset

The third phase looked at the sensors' transverse sensitivity to offset forces, using 4 different applied force directions (30°, 45°, 60°, 90°) to compare against the inline force direction response (0°). Figures 12 and 13 show the general trend of sensor response for the coverstitch and chainstitch groups (regardless of fabric substrate and sensor angle placement), while comparison charts of the GF and K_T for all sample groups are shown in Figures 14 and 15, respectively. The hysteresis error, R^2 and RMSE values are presented in text.

As Figure 14 shows, there is still 50+% GF observed for forces applied 30° from the sensor (1st column in each group/red) which decreases as the force direction angle approaches 90°. The exception is the 2-way coverstitch sample groups which have an opposite trend, potentially due to unequal stiffness causing increased sensor response when the fabric is pulled in the less stiff fabric directions.

However, this decreasing trend is non-uniform and its magnitude is influenced by the sensor geometry. The coverstitched sensor groups still maintain 30+% sensitivity that is relatively uniform for all offset forces except in the 4-way coverstitch @0° group (Figure 13). The chainstitched sensor groups have a more marked decrease (Figure 12), often falling to ~ 0 when subjected to 60° and 90° offset force directions, which is desirable in a strain sensor. Of the chainstitch groups, the 4-way knit sensors were affected more by offset forces than the 2-way knit sensors.

According to the traditional strain sensor design, the transverse sensitivity is derived from the measured sensitivity when force is applied perpendicular to the sensor axis. Interestingly, the lowest

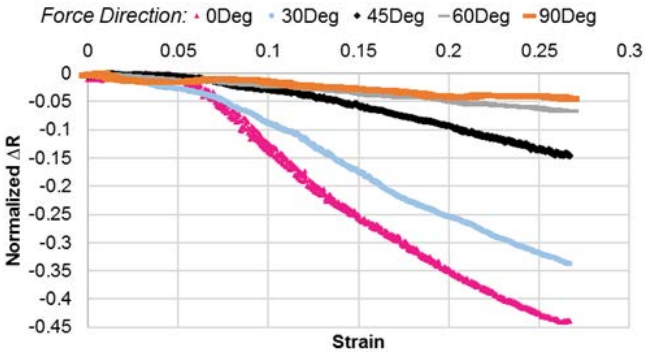

Figure 12: 4-way Chainstitch Sensor: Normalized Δ Resistance vs Strain (Sensor sewn 30° onto knit). Reprinted from [21]

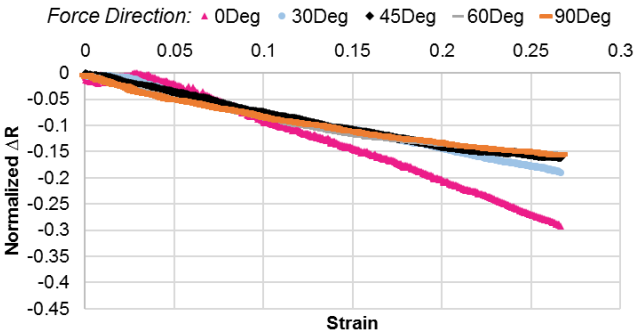

Figure 13: 4-way Coverstitch Sensor: Normalized Δ Resistance vs Strain (Sensor sewn 30° onto knit). Reprinted from [21]

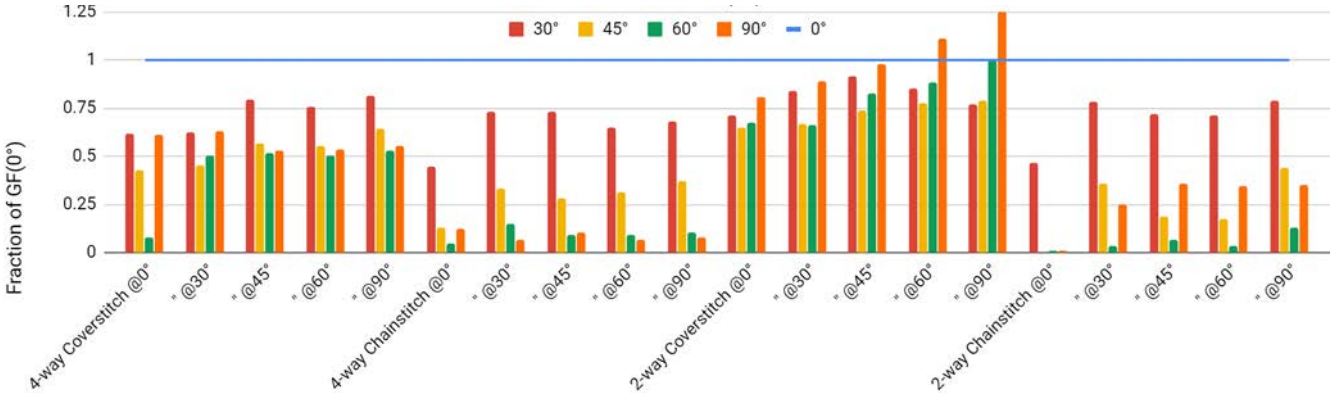

Figure 14: Sensor Sensitivity to Offset Forces (gauge factor of each applied strain direction divided by the 0° force direction gauge factor). Reprinted from [21]

sensitivity across the entire set of applied force directions was found to be mainly 60° (Figure 14, 3rd column in each group/green). This effect is probably due to the horizontal widening of the stitch sensor inducing a greater sensor response in the 90° offset force direction than in the 60° direction. Consequently, the comparison of transverse sensitivity using the 60° direction (Figure 15) shows an advantage of the chainstitch over the coverstitch sensor geometry, although the coverstitch shows lower values on the 4-way knit vs the 2-way knit.

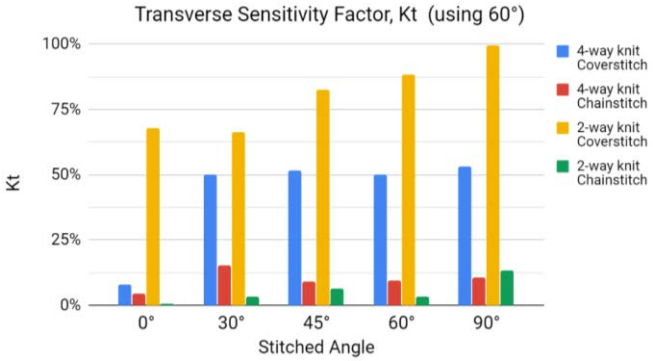

Figure 15: Transverse Sensitivity Factor of Stitched Sensors. Reprinted from [21]

In summary, the wider coverstitched sensor geometry shows higher overall sensitivities to offset forces and high K_T values. The low K_T values seen for the chainstitched sensor geometry suggests it could perform well at measuring force directionality, for example in strain rosette designs.

Due to increased variability in the sensor response (more so with the chainstitch groups) as the offset angle of the force direction increased from 30° to 90°, the R^2 values decreased from an average value of 0.95 for inline force to 0.83 for offset forces. The baseline drift was minimal (avg -0.02Ω) and smaller than the values seen for the sensor responses of inline force (avg -0.10Ω). The hysteresis error for offset sensor responses averaged higher (5% to 16%) than those seen for the inline sensor response for the coverstitched sensors and 0° stitch angles, and slightly lower (-6% to 10%) for chainstitched sensors and the other stitch angles.

4 Conclusion

This investigation highlights the impact of fabric substrate mechanical properties, sensor geometry, and sensor orientation on the electro-mechanical sensor performance of a conductive stitched strain sensor. Algorithms that help smooth noisy data and normalize measurements to nominal data are still useful, but key design choices in fabricating a stitched strain sensor can reduce error and improve the analysis of predicted force, elongation, and force direction before data is even conditioned.

The conductive stitched strain sensor was previously determined to have a linear response but the results presented here showcase how the linear mechanical response can become non-linear and even exponential depending on the fabric knit substrate selection and angle of applied uniaxial force. The sensor responses in stiffer directions of the 2-way knit were so curved that a linear fit is no longer recommended (this is not to say that this combination is unusable, simply that a linear model can't be assumed). Future testing could confirm whether 2-way knits consistently produce exponential sensor responses and if exponential models should be used for these applications. If the application requires sensing larger forces (>50N), then a stiffer knit fabric would be recommended.

The 4-way knit substrate allowed easier comparison of sensors stitched at various angles and produced more consistent sensor performance. (To note, the elastic content, Lycra™/Spandex™, of the 4-way knit afforded better repeatability and would be considered to be a prerequisite to selecting appropriate fabric substrates to use with these sensors [13]). In general, for most smart wearable garment applications, an elastic 4-way knit fabric with relatively similar mechanical behavior in the 0° and 90° directions would be recommended for these stitched sensors or similar designs.

Using 7cm sensors, strains up to ~30% (2cm displacement) were applied by a tensile tester. Analysis of the sensor response showed that a change in resistance typically began at ~5mm (7%), continued until 30%, and ended again at ~5mm. Additional testing could confirm the upper limit, but both sensor geometries proved repeatable in this strain range. The normalized peak-to-peak ΔR was higher for the chainstitch geometry (~46%) than the coverstitch (~27%), resulting in a higher GF.

Although variation was observed in the elastic moduli, the sensor orientation/stitched angle of the sensor relative to the fabric induced little variation in the sensor's gauge force, linearity error R^2, RMSE, and hysteresis error. More variation was induced by combined factors of stiffness between the sensor geometry and the fabric property: for example, the wider coverstitch geometry on the 2-way fabric. The baseline drift decreased from the stiffest to the stretchiest fabric direction, and sensor placement did seem to have an effect on this performance variable. The presence of elasticity allowed for greater recovery and lower drift values. The hysteresis error was greater for the chainstitched sensor geometry than the coverstitch, presenting a trade-off with its higher GF values.

The coverstitch geometry was much more sensitive to offset forces than the chainstitch geometry. The high transverse sensitivity factor, K_T, for the coverstitch geometry indicates that even a single sensor would be sufficient at sensing in-plane forces applied in any direction but it would be difficult to distinguish the direction of force applied. This is opposite for the chainstitched sensor, where the K_T is very low, and suited to applications that desire predicting force directionality.

The 4-way knit had greater overall consistency over the 2-way knit; however, if the application necessitates a high force range, the 2-way knits can structurally support this. The mechanical properties do result in a range of potential elastic modulus values that complicate absolute force predictions, but this does not seem to

result in a range of sensor GF. The advantages of the coverstitch geometry are a greater sensitivity to offset forces, higher linearity R^2, lower RMSE, and smaller hysteresis error. The advantages of the chainstitch geometry are a greater GF, lower sensitivity to offset forces, and lower baseline drift. Each has recommended uses: for detecting the presence of 2-D plane forces/strains, a coverstitched sensor stitched on a 4-way knit's least stiff direction (90°) may be recommended, whereas for distinguishing individual force directions, multiple chainstitched sensors on a 4-way knit would be recommended.

Using stitched sensors coupled to knit textiles can add complexity to the design of a wearable sensor system, but adequate characterization of the interaction between sensor and textile mechanics can inform system design and improve overall performance of textile-based sensors without sacrificing user comfort.

ACKNOWLEDGMENTS

This work was supported in part by the US National Science Foundation under grant #1722738.

AUTHOR CONTRIBUTIONS

Ellen Dupler contributed sensor design, study strategy and methodology, sample preparation, data collection, statistical analysis, and preparation of the manuscript. Dr. Lucy Dunne contributed to sensor design, study strategy and methodology, and preparation of the manuscript.

REFERENCES

1. Morteza Amjadi, Ki-Uk Kyung, Inkyu Park, and Metin Sitti. 2016. Stretchable, Skin-Mountable, and Wearable Strain Sensors and Their Potential Applications: A Review. *Advanced Functional Materials* 26, 11: 1678–1698. https://doi.org/10.1002/adfm.201504755
2. Ozgur Atalay and William Richard Kennon. 2014. Knitted Strain Sensors: Impact of Design Parameters on Sensing Properties. *Sensors (Basel, Switzerland)* 14, 3: 4712–4730. https://doi.org/10.3390/s140304712
3. Ozgur Atalay, William Richard Kennon, and Muhammad Dawood Husain. 2013. Textile-Based Weft Knitted Strain Sensors: Effect of Fabric Parameters on Sensor Properties. *Sensors* 13, 8: 11114–11127. https://doi.org/10.3390/s130811114
4. Lina M. Castano and Alison B. Flatau. 2014. Smart fabric sensors and e-textile technologies: a review. *Smart Materials and Structures* 23, 5: 053001. https://doi.org/10.1088/0964-1726/23/5/053001
5. A Ehrmann, F Heimlich, A Brücken, MO Weber, and R Haug. 2014. Suitability of knitted fabrics as elongation sensors subject to structure, stitch dimension and elongation direction. *Textile Research Journal* 84, 18: 2006–2012. https://doi.org/10.1177/0040517514548812
6. Jonny Farringdon, Andrew J. Moore, Nancy Tilbury, James Church, and Pieter D. Biemond. 1999. Wearable Sensor Badge and Sensor Jacket for Context Awareness. In *ISWC*, 107–113. Retrieved from http://citeseer.ist.psu.edu/farringdon99wearable.html
7. G. Gioberto, J. Coughlin, K. Bibeau, and L. E. Dunne. 2013. Detecting bends and fabric folds using stitched sensors. In *Proceedings of the 14th International Symposium on Wearable Computers*.
8. Guido Gioberto, C. Compton, and L. E. Dunne. 2016. Machine-Stitched E-Textile Stretch Sensors. *Sensors and Transducers Journal* 202, 7: 25–37.
9. Guido Gioberto and Lucy E. Dunne. 2013. Overlock-Stitched Stretch Sensors: Characterization and Effect of Fabric Property. *Journal of Textile and Apparel, Technology and Management* 8, 3. Retrieved March 15, 2014 from http://ojs.cnr.ncsu.edu/index.php/JTATM/article/view/4417
10. Guido Gioberto, Cheol-Hong Min, Crystal Compton, and Lucy E. Dunne. 2014. Lower-limb Goniometry Using Stitched Sensors: Effects of Manufacturing and Wear Variables. In *Proceedings of the 2014 ACM International Symposium on Wearable Computers* (ISWC '14), 131–132. https://doi.org/10.1145/2634317.2634336
11. Ching-Tang Huang, Chien-Fa Tang, and Chien-Lung Shen. 2006. A Wearable Textile for Monitoring Respiration, Using a Yarn-Based Sensor. In *2006 10th IEEE International Symposium on Wearable Computers*, 141–142. https://doi.org/10.1109/ISWC.2006.286366
12. Y. Liu, L. Xu, Y. Li, and T. T. Ye. 2019. Textile Based Embroidery-Friendly RFID Antenna Design Techniques. In *2019 IEEE International Conference on RFID (RFID)*, 1–6. https://doi.org/10.1109/RFID.2019.8719270
13. F. Lorussi, W. Rocchia, E. P. Scilingo, A. Tognetti, and D. De Rossi. 2004. Wearable, redundant fabric-based sensor arrays for reconstruction of body segment posture. *IEEE Sensors Journal* 4, 6: 807–818.
14. C. Mattmann, O. Amft, H. Harms, G. Troster, and F. Clemens. 2007. Recognizing Upper Body Postures using Textile Strain Sensors. In *Wearable Computers, 2007 11th IEEE International Symposium on*, 29–36. https://doi.org/10.1109/ISWC.2007.4373773
15. E. Moradi, T. Bjorninen, L. Ukkonen, and Y. Rahmat-Samii. 2012. Effects of Sewing Pattern on the Performance of Embroidered Dipole-Type RFID Tag Antennas. *IEEE Antennas and Wireless Propagation Letters* 11: 1482–1485. https://doi.org/10.1109/LAWP.2012.2231393
16. Anita Vogl, Patrick Parzer, Teo Babic, Joanne Leong, Alex Olwal, and Michael Haller. 2017. StretchEBand: Enabling Fabric-based Interactions Through Rapid Fabrication of Textile Stretch Sensors. In *Proceedings of the 2017 CHI Conference on Human Factors in Computing Systems* (CHI '17), 2617–2627. https://doi.org/10.1145/3025453.3025938
17. R. Wijesiriwardana, T. Dias, and S. Mukhopadhyay. 2003. Resistive Fibre-Meshed Transducers. In *Proceedings of the 7th IEEE International Symposium on Wearable Computers* (ISWC '03), 200–. Retrieved May 2, 2012 from http://dl.acm.org/citation.cfm?id=946249.946872
18. R. Wijesiriwardana, K. Mitcham, and T. Dias. 2004. Fibre-meshed transducers based real time wearable physiological information monitoring system. In *Eighth International Symposium on Wearable Computers*, 40–47. https://doi.org/10.1109/ISWC.2004.20
19. Hui Zhang, Xiaoming Tao, Shanyuan Wang, and Tongxi Yu. 2005. Electro-Mechanical Properties of Knitted Fabric Made From Conductive Multi-Filament Yarn Under Unidirectional Extension. *Textile Research Journal* 75, 8: 598–606. https://doi.org/10.1177/0040517505056870
20. Rui Zhang, Martin Freund, Oliver Amft, Jingyuan Cheng, Bo Zhou, Paul Lukowicz, Seoane Fernando, and Peter Chabrecek. 2016. A Generic Sensor Fabric for Multi-modal Swallowing Sensing in Regular Upper-body Shirts. In *Proceedings of the 2016 ACM International Symposium on Wearable Computers* (ISWC '16), 46–47. https://doi.org/10.1145/2971763.2971785
21. E. Dupler. (2019). Characterizing the Influence of the Textile-Sensor Interface on Stitched Sensor Performance. Master's thesis. University of Minnesota, USA.